# Fluorescence Property of Polycarbonate Related to Radial-Pattern Formation

**M. Tanimura,[1] M. Tachibana,[2] K. Kojima[2]**

[1]*Research Department, NISSAN ARC, Ltd., 1 Natsushima-cho, Yokosuka 237-0061, Japan*
[2]*Graduate School of Integrated Science, Yokohama City University 22-2 Seto, Kanazawa-ku, Yokohama 236-0027, Japan*

Received 25 July 2003; accepted 20 October 2003

**ABSTRACT:** The pattern change in a laminar flow of molten polycarbonate in a disk mold was experimentally investigated by altering the flow velocity. By use of a light-scattering method, a radial pattern characterized by a periodic array of needlelike regions and the matrix was found to form as the flow velocity was increased. The density distribution of the polycarbonate molecules was an essential factor for pattern formation. As a result of the formation of this pattern, it was found that the boundaries between the needlelike regions and the matrix emitted weak fluorescence in the wavelength range of 600–700 nm under laser irradiation. An analysis indicated that transitions between excited $\pi$ electron states in the phenylene groups were the sources of this fluorescence and that a key factor behind its occurrence was a decrease in the molecule density at the boundaries. These results reveal that the radial-pattern formation changes the fluorescence property of polycarbonate in the visible and near-infrared regions. © 2004 Wiley Periodicals, Inc. J Appl Polym Sci 92: 468–473, 2004

**Key words:** polycarbonate; injection molding; pattern formation; fluorescence

## INTRODUCTION

Polymer products made by injection molding exhibit a variety of patterns depending on their fabrication conditions. It is well known that variation of the injection-molding conditions causes pattern changes that produce differences in the physical properties of polymer products. The relation between pattern formation and functionality is therefore an important issue for polymer products to obtain the target properties.

Recently, we found that a radial pattern appears in the polycarbonate (PC) substratum of optical disks.[1] This radial pattern is characterized as a periodic array of needlelike regions having a thin film shape and the matrix in the radial direction of the disks. It is noteworthy that the density of PC molecules decreases at the boundaries between the needlelike regions and the matrix, which implies that the periodic density distribution of PC molecules is essential to form the radial pattern. As is well known, the PC substratum is made by an injection-molding process in which the molten PC is injected from the center of the disk mold, followed by rapid cooling to room temperature.[2,3] Thus, the formation of such a pattern is of high interest in terms of the flow dynamics of the molten PC in the disk mold. In addition, the PC substratum is required to have good transparency to the laser beam that is utilized to record and play back the sound and images on an optical disk. Our interest is therefore focused on the relation between the radial-pattern formation and the change in the optical response of PC disks to laser irradiation because of the density distribution of PC molecules.

In this article, we will describe the change in the patterns observed experimentally for PC disks in relation to the change in the injection conditions. Because one important parameter controlling the molten-PC flow in the disk mold is the flow velocity in the injection-molding process, the change in the patterns was induced by altering the velocity. We further show that weak fluorescence is emitted from the boundaries between the needlelike regions and the matrix in the radial pattern under irradiation by a visible laser beam. These experimental results clearly indicate an example where the pattern appearing in a PC disk actually changes the optical properties of PC products. The details of the experimental conditions and the results will be described below.

## EXPERIMENTAL

PC powder with an average molecular weight of about 15,000 was melted at 573 K. Figure 1 shows schematic diagrams of the injection-molding system used in the present work and the flows of the molten PC in planar and cross-section views. Molten PC is injected from the center of the disk mold, extends in the radial direction, and then spreads along the circumference of the mold, as shown in Figure 1(a). It is

*Correspondence to:* M. Tanimura (tanimura@nissan-arc.co.jp).

Journal of Applied Polymer Science, Vol. 92, 468–473 (2004)

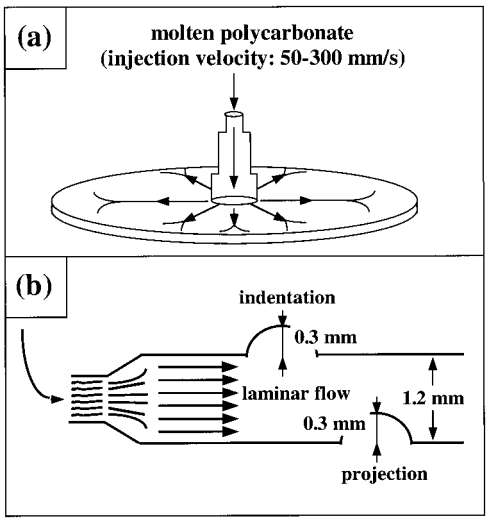


**Figure 1** Schematic diagrams of (a) the molten PC flow in the disk mold, and (b) the flow as seen in a cross section of the mold. The marks of the stamper are denoted, respectively, as an indentation and a projection at the upper and lower surface planes of the disk mold in (b).

known that the kinematic viscosity of molten PC is about 1.0 $m^2/s$ at 573 K and that it is nearly independent of the shear velocity near this temperature.[2,3] Thus, the present flow can be regarded as laminar flow having a Newtonian nature. The radial flow in a cross section is depicted in Figure 1(b). Note that an indentation and a projection are present at the upper and lower surface planes of the disk mold, which correspond to the marks of the stamper used to support the molded disk. Injection velocities were varied in a range of 50–300 mm/s.

The appearance of the pattern in the molten PC flow was detected as follows. To freeze the pattern in the flow, the disk mold was rapidly cooled to room temperature after injection of the PC melt was finished. Because the molecule density distribution is an essential factor in the formation of the pattern, a light-scattering method is appropriate for pattern detection. The PC disks were irradiated by a halogen lamp having its main spectrum at 365 nm, and optical micrographs of the pattern were taken with a charge-coupled device camera by using the scattered light from the PC disks. In the observation, a band-pass filter was used to catch effectively the light scattered from the PC disks.

Fluorescence spectra were measured by using both a Nd-YAG laser (532 nm) and a He-Cd laser (442 nm) as the incident beam together with a photodiode-grating system. Because the normal thickness of the needlelike regions is less than 0.1 mm, flat planes were made by polishing the PC disks to a thickness of about 0.1 mm. Cross sections for the measurement were obtained by cutting the PC disks into a size of about 10 $\times$ 5 $\times$ 1 $mm^3$.

## RESULTS

### Formation of the radial pattern

First of all, we will explain the change observed in the flow pattern in the disk mold by altering the flow velocity. Figure 2 shows optical micrographs of the flat planes of the PC disks. The disks were fabricated by injecting molten PC at a velocity of 50 mm/s in Figure 2(a), 150 mm/s in Figure 2(b), and 300 mm/s in Figure 2(c), respectively. These disks will be referred to here as the 50-disk, the 150-disk, and the 300-disk, respectively. In the flat plane shown in Figure 2(a), no pattern can be detected in the 50-disk. This indicates that the density of the PC molecules did not fluctuate in the disk to the extent that the incident light was scattered. Note that PC has good transparency to visible and near-infrared light when it has a uniform density distribution. In the micrograph in Figure 2(b), on the other hand, periodic needlelike regions of about

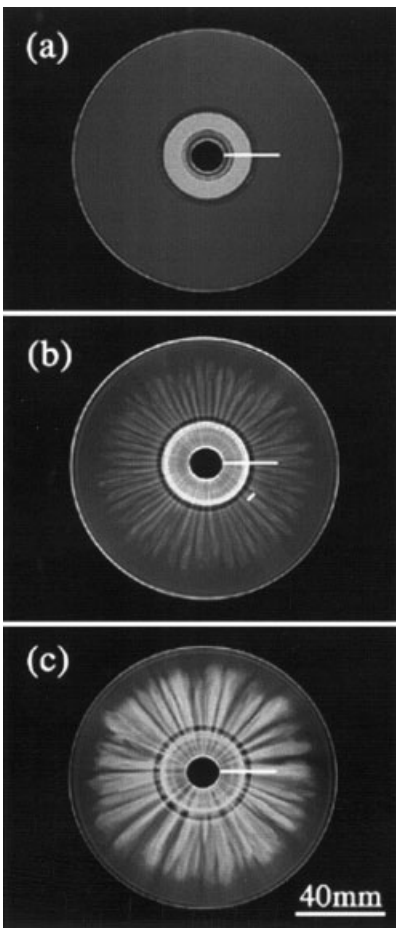


**Figure 2** Optical micrographs of the flat planes of PC disks fabricated at injection velocities of (a) 50 mm/s, (b) 150 mm/s, and (c) 300 mm/s, respectively. These micrographs were taken by using light scattered from the disks. Radial patterns composed of needlelike regions can be observed in the 150- and the 300-disks, while no pattern is detected in the 50-disk.

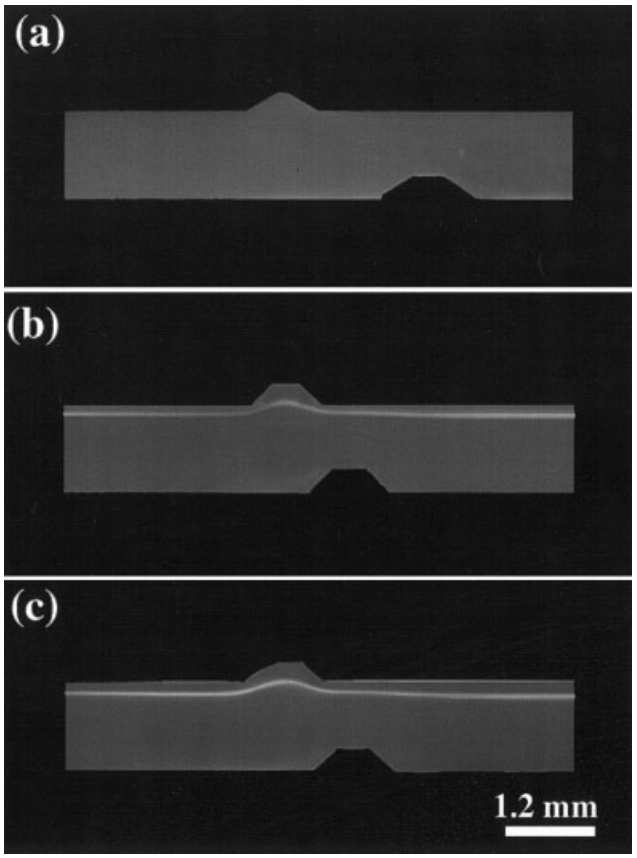


**Figure 3** Optical micrographs of the cross sections of PC disks fabricated at the injection velocities of (a) 50 mm/s, (b) 150 mm/s, and (c) 300 mm/s, respectively. Band-shaped regions around the indentation are observed only in the 150- and the 300-disks. From an analysis of the contrast, the band-shaped regions correspond to the needlelike regions shown in the flat planes.

2 mm in width are observed near the center hole. The end of the regions corresponds to the point where the flow direction changes from radial to circumferential. An important feature is that each needlelike region gives rise to bright contrast, while the matrix exhibits dark contrast. As was reported in our previous article,[1] the boundaries surrounding the needlelike regions scattered the light and the wavelength of the scattering light was 400–680 nm (white light). The number of the needlelike regions is about 70, with each region extending in the radial direction from the center hole. The radial pattern can also be detected in the 300-disk shown in Figure 2(c). An important difference from the 150-disk is that the number of the needlelike regions of the 300-disk is reduced to about 40, with each needlelike region being wider (about 3 mm) around the center hole. From these experimental results, it is understood that the critical velocity needed to form the radial pattern is about 100 mm/s.

An observation of cross sections along the radial direction of the disks was also carried out. Figure 3 shows the cross sections of the three types of disk. The locations of the cross sections are indicated by the long lines shown in Figure 2. In the 50-disk, no characteristic pattern can be detected, as seen in Figure 3(a), which can be expected from the result shown in Figure 2(a). In the cross section of the 150-disk shown in Figure 3(b), a band-shaped region with a thin film shape (the width was less than 0.1 mm) exists around the indentation, 200 $\mu$m below the upper surface. Because the band-shaped region exhibits bright contrast due to light scattering, the region is understood to correspond to one of the needlelike regions shown in the flat plane. Thus, it is confirmed that the needlelike regions have a thin film shape. A band-shaped region corresponding to one needlelike region with a thin film shape also formed in the cross section of the 300-disk [Fig. 3(c)]. The region in the 300-disk displays almost the same features as that in the 150-disk. This implies that the height of the needlelike regions is independent of the injection velocity and that the laminar nature of the molten-PC flow is preserved when the velocity of the flow increases to 300 m/s.

### Fluorescence emission

Because the appearance of the radial pattern was detected in the 150- and the 300-disks, the optical behavior of these disks was examined under laser irradiation. Figure 4(a) shows a micrograph of a cross section perpendicular to the radial direction of the 150-disk. The micrograph was taken by irradiating the disk with the Nd-YAG laser (532 nm) and the location of the cross section is indicated by a short line in Figure 2(b). We can see in the micrograph that only the boundary between the needlelike region and the matrix exhibits bright contrast. To examine the light giving rise to this bright contrast at the boundaries, the light wavelengths were measured when the Nd-YAG laser irradiated the boundaries and the matrix. Figure 4(b) shows the spectra obtained from both a boundary, labeled as NY-**B**, and the matrix, labeled as NY-**M**, in the cross section of the 150-disk. The measured locations are indicated in Figure 4(a). As can be seen in Figure 4(b), there are no conspicuous peaks between 550 and 750 nm in the spectrum obtained from the matrix, indicating that no light was scattered there. On the other hand, there exist major sharp peaks at 628 and 709 nm as well as minor peaks at 597 and 617 nm in the spectrum from the boundary, although the intensities of all peaks are very weak. The detection of these peaks implies that the boundary contrast shown in Figure 4(a) originates from light rays at these wavelengths. It should be mentioned here that the existence of these four peaks was also confirmed by measuring the spectra in the flat plane of the 150-disk. From these results, it is obvious that the boundaries and the ma-

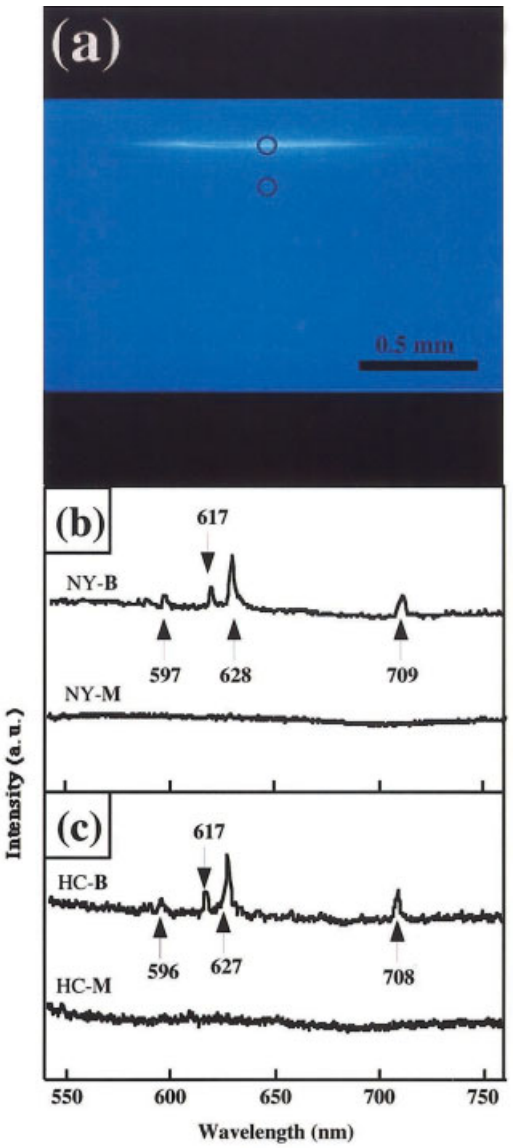


**Figure 4** (a) Optical micrographs of a cross section obtained by YAG laser irradiation. Only the boundary between a needlelike region and the matrix gives rise to bright contrast. (b) Fluorescence spectra of the cross section of the 150-disk obtained under Nd-YAG laser irradiation. The notations NY-**B** and NY-**M** denote a boundary and the matrix, respectively. Four weak and sharp peaks can be seen in the spectrum diagram. (c) Fluorescence spectra of the same sample obtained under He-Cd laser irradiation, where HC-**B** and HC-**M** indicate a boundary and the matrix. Four peaks having the same wavelengths as those in (b) are detected in the diagram.

trix in the PC disk responded differently to laser irradiation.

To determine the origin of the peaks appearing at the boundaries, measurements were also made by changing the wavelengths of incident light (He-Cd laser; 442 nm). Figure 4(c) shows the spectra obtained from the boundary (HC-**B**) and the matrix (HC-**M**) in the cross section of the 150-disk. The locations of the measurements are the same as those in the case of Nd-YAG laser irradiation. In the spectrum obtained from the boundary, sharp peaks are observed at 596, 617, 627, and 708 nm, whereas no peaks can be detected in the spectrum from the matrix. An important feature of the peaks is that the wavelengths are consistent with those of the peaks obtained by Nd-YAG laser irradiation. This implies that the locations where the peaks appear are basically independent of the wavelength of incident light. Thus, it is understood that these peaks are caused by fluorescence, rather than by light scattering such as Raman scattering. Considering that the normal wavelength of the fluorescence emitted from standard PC is about 320 nm,[4–9] this fluorescence can be regarded as the effect of the formation of boundaries with a low molecule density due to the formation of the radial pattern. It should be mentioned here that the appearance of four fluorescence peaks having the same features was confirmed in the 300-disk, whereas no peaks were detected from the 50-disk.

## DISCUSSION

### Pattern change in the molten-PC flows

The experimental results revealed that the radial pattern formed with an increase in the injection velocity. This implies that the pattern changes in the laminar flow of molten PC in the disk mold under the present injection conditions. We will characterize here the present flow based on an estimation of the Reynolds number (Re), which describes the bifurcation in the flow of micromolecules (e.g., air and water),[10] although the large degree of internal freedom of the molecules making up the fluid complicates the flow dynamics.[11–16] The calculated Re of the flow around the center hole is on the order of $10^{-5}$ at an injection velocity of 50 mm/s and on the order of $10^{-4}$ at 300 mm/s. These estimations are based on the relation $\mathrm{Re} = vs/\eta_T$, where $v$, $s$, and $\eta_T$ are the flow velocity, the height of the disk mold, and the kinematic viscosity of the flow at temperature $T$, respectively. (Strictly, the flow velocity is smaller than the injection velocity. However, the nature of the flow can be inferred by applying the latter velocity to the former one.) The calculated values indicate that the present flow can be approximated as Stokes flow. Because the critical Re needed to form the radial pattern is about $10^{-4}$, the estimations reveal the occurrence of a pattern change even in Stokes flow. In general, the Stokes approximation can only be applied to flows by treating the viscous term and ignoring the contribution of the inertia term. Thus, the pattern in Stokes flow should be basically independent of the change in Re. However, the present estimations suggest a possibility of pattern bifurcation in the low Re region. This can therefore

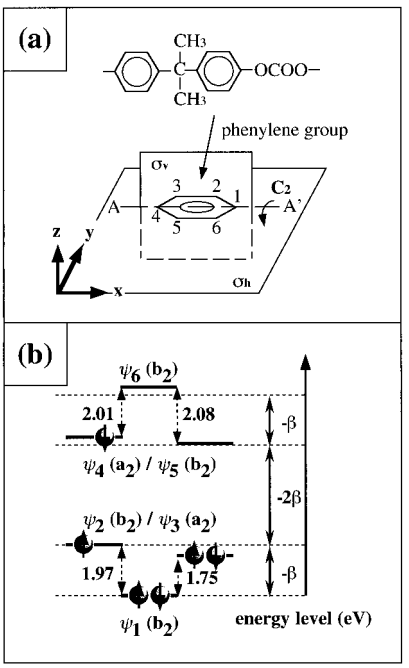


**Figure 5** (a) Schematic diagram of the PC molecule structure. The symmetry elements of the phenylene group are $E$, $C_2$, $\sigma_h$, and $\sigma_v$ and its point group is determined to be $C_{2[infi]v}$. (b) Schematic diagram of the energy level and the representation of the $\pi$ state of the phenylene group that emits the present fluorescence.

pose an interesting issue for pattern formation in a macromolecule flow from the viewpoint of fluid dynamics. However, we will not delve so deeply into this issue in this article. A detailed analysis based on a simulation of the PC-flow dynamics in the disk mold will be reported elsewhere.[17]

### Electron transition causing the fluorescence

In general, fluorescence is produced by an electron transition. In the case of aromatic compounds, the $\pi \Rightarrow \pi^*$ electron transition in a benzene ring plays a crucial role in the emission of fluorescence.[18,19] In line with this viewpoint, we will note the $\pi$ state of a phenylene group present in the PC monomer based on a $\pi$ electron approximation. Figure 5(a) shows the structural diagram of PC, together with the symmetry elements, the axes of the coordinates, and the index $n$ (1–6) for carbons of a phenylene group. As is evident from the diagram, the point group of the phenylene group is $C_{2v}$. When we give six $p_z$ atomic orbits of six carbons as a set of the basis, the irreducible representations of the basis are found to be $2a_2 + 4b_2$. It should be noted that all of the electron states belong to either the $A_1$ or the $B_1$ representations. Thus, an electron transition between two states may be any one of $A_1 \Leftrightarrow A_1$, $A_1 \Leftrightarrow B_1$, or $B_1 \Leftrightarrow B_1$, all of which are the allowed transitions in terms of the selection rule. We can now obtain the representation and the energy level of each molecular orbit of a phenylene group as follows: $\psi_1(b_2, \alpha + 2\beta)$, $\psi_2(b_2, \alpha + \beta)$, $\psi_3(a_2, \alpha + \beta)$, $\psi_4(a_2, \alpha - \beta)$, $\psi_5(b_2, \alpha - \beta)$, and $\psi_6(b_2, \alpha - 2\beta)$. For simplicity, only the effect of the neighboring carbons is taken into account in the calculation, and the overlap integral is ignored for the estimation of the energy levels [i.e., $H_{ij} = \alpha$ $(i = j)$, $\beta$ $(i = j \pm 1)$, and 0 (others), while $S_{ij} = 1$ $(i = j)$ and 0 $(i \neq j)$, where $H_{ij}$ and $S_{ij}$ are the Coulomb integral and the overlap integral, respectively. It should be noted that both the $\psi_2 - \psi_3$ and the $\psi_4 - \psi_5$ molecular orbits seem to be degenerate. This degeneration, however, is removed when the electron correlation is taken into account more strictly and it is assumed that the energy levels of the molecular orbits have shifted.

We will qualitatively assign the electron transition that produces fluorescence. Because the fluorescence of standard PC, having a wavelength of about 320 nm, is caused by the transition between the ground state and the lowest excited state,[4–9] [e.g., $(\psi_1)^2(\psi_2)^2(\psi_3)^1(\psi_4)^1 \Rightarrow (\psi_1)^2(\psi_2)^2(\psi_3)^2$], the energy gap between these two states, $-2\beta$, is about 3.88 eV. Thus, the wavelength of fluorescence originating from electron transitions having an energy gap of $-\beta$ (1.94 eV) should be about 640 nm. Actually, the observed wavelengths are 597 nm (2.08 eV), 617 nm (2.01 eV), 628 nm (1.97 eV), and 709 nm (1.75 eV). From the good correspondence of these energy values with $-\beta$, we can identify the sources of the four observed fluorescence peaks as being the transitions, including $\psi_2 \Rightarrow \psi_1$, $\psi_3 \Rightarrow \psi_1$, $\psi_6 \Rightarrow \psi_4$, and $\psi_6 \Rightarrow \psi_5$. Because the intensities due to the $\psi_6 \Rightarrow \psi_4$ and $\psi_6 \Rightarrow \psi_5$ transitions within the antibonding orbital must be very weak, the minor fluorescence spectra located at 597 and 617 nm originate from these transitions, whereas the major peaks at 628 and 709 nm are due to the $\psi_2 \Rightarrow \psi_1$ and $\psi_3 \Rightarrow \psi_1$ transitions within the bonding orbital. On the basis of this assignment, a schematic diagram of the electronic structure of the $\pi$ state causing the present fluorescence is shown in Figure 5(b).

### Relation between fluorescence emission and radial-pattern formation

Finally, we will discuss the relation between the formation of the radial pattern and the appearance of the fluorescence property in the PC disks. Our experimental results reveal that the radial pattern forms when the injection velocity increases; in other words, the contribution of the viscous term becomes small in the laminar flow. This indicates that the boundaries with low molecule density are produced by the separation of the laminar flow due to the small viscous term contribution, followed by rapid cooling to room temperature. Because the boundaries can be regarded as a metastable state formed by rapid cooling, their electronic structure can have a larger number of states of a high-energy electron configuration [e.g., $(\psi_1)^2(\psi_2)^2(\psi_3)^1(\psi_4)^1$] in the $\pi$ state of

the phenylene group than that of the matrix. On the other hand, the above-mentioned analysis indicates that four electron transitions between the excited electron states in the phenylene group play a crucial role in the emission of fluorescence. In order for these transitions to occur, the $\psi_2$ and/or $\psi_3$ molecular orbit must not be fully occupied, while one electron at least must exist in the $\psi_4$ and/or $\psi_5$ molecular orbits in the initial state [see Fig. 5(b)]. These conditions imply that the boundaries are in a state conducive to the occurrence of these four electron transitions under laser irradiation and can play a role in forming the color center of the emission. Ultimately, the radial pattern formed in the PC disks changes its fluorescence property by controlling the electronic structure of the $\pi$ state of the phenylene group in PC molecules.

## CONCLUSION

In this study, the relation between pattern formation and property changes in PC was experimentally investigated. It was found that the flow pattern of molten PC in the disk mold changed even in the low Re region and that a radial pattern having a periodic array of needlelike regions and the matrix formed when the flow velocity was increased above 100 mm/s. In connection with the formation of this radial pattern, weak fluorescence was emitted in the wavelength range of 600–700 nm from the boundaries between the needlelike regions and the matrix under YAG (532 nm) and He-Cd (442 nm) laser irradiation. An analysis indicated that transitions between excited $\pi$ electron states in the phenylene groups were the sources of this fluorescence, which originated from the high-energy electron configuration of boundaries having a low molecule density. In conclusion, the formation of this radial pattern in PC disks contributes to the appearance of a new property related to the density distribution of PC molecules, a manifestation of which is fluorescence emitted from the boundaries between the needlelike regions and the matrix.

One of the authors (M.T.) acknowledges the technical support of I. Ishikawa and T. Okamura (NISSAN ARC, Ltd.).

## References

1. Tanimura, M.; Ishikawa, I.; Tachibana, M.; Shinozaki, K.; Kojima, K. Appl Phys Lett 2001, 79, 1778.
2. Yoshioka, H. in Kagaku Sousetu (Outline of Chemistry); Chemical Society of Japan, Ed.; Vol. 39, 1998; Chapter 9.
3. Ohyanagi, Y. Engineering Plastics, 1st ed.; Morikita: Tokyo, 1985.
4. Rivaton, A.; Sallet, D.; Lemaire, J. J Polym Degrad Stab 1986, 14, 1.
5. Factor, A.; Ligon, W. V.; May, R. J. Macromolecules 1987, 20, 2461.
6. Hoyle, C. E.; Shah, H.; Nelson, G. L. J Polym Sci, Part A: Polym Chem 1992, 30, 1525.
7. Shah, H.; Rufus, I. B.; Hoyle, C. E. Macromolecules 1994, 27, 553.
8. Lee, L. H. Polym Sci, Part A: Polym Chem 1964, 2, 2859.
9. Montaudo, G.; Puglisi, C. J Polym Degrad Stab 1992, 37, 91.
10. Reynolds, O. Philos Trans R Soc 1883, 174, 935.
11. Shore, J. D.; Roins, D.; Piche, L.; Grant, M. Phys Rev Lett 1996, 77, 655.
12. Black, W. B.; Graham, M. D. Phys Rev Lett 1996, 77, 956.
13. Groisman, A.; Steinberg, V. Phys Rev Lett 1996, 77, 1480.
14. Hobbie, E. K.; Kim, S.; Han, C. C. Phys Rev E 1996, 54, R5909.
15. Shore, J. D.; Roins, D.; Piche, L.; Grant, M. Phys Rev E 1997, 55, 2976.
16. Likhtman, A. E.; Milner, S. T.; McLeish, T. C. B. Phys Rev Lett 2000, 85, 4550.
17. Tanimura, M. to appear.
18. Haken, H.; Wolf, H. C. Molecular Physics and Elements of Quantum Chemistry; Springer: Stuttgart, 1995.
19. Montanari, B.; Ballone, P.; Jones, R. Macromolecules 1999, 32, 3396.